

# Transport of Galactic Cosmic-Ray Nuclei

Benedikt Schroer

Carmelo Evoli, Pasquale Blasi

May 16, 2023



THE UNIVERSITY OF  
CHICAGO

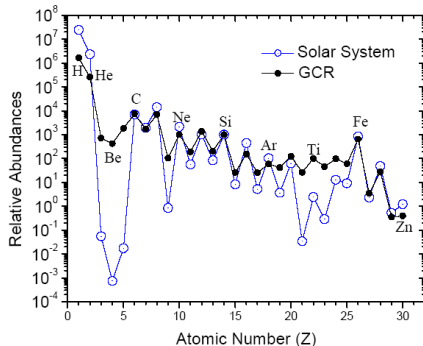
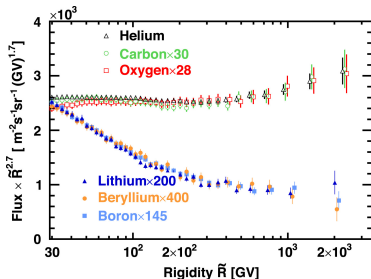
- 1 Introduction
- 2 Weighted Slab Model
- 3 Lighter Nuclei
- 4 Intermediate-mass and Heavy Nuclei
- 5 Conclusion and Outlook



# Introduction



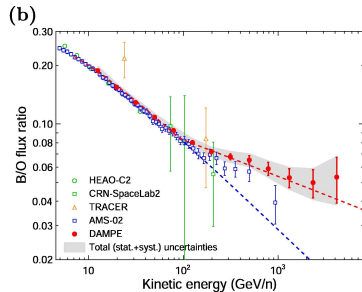
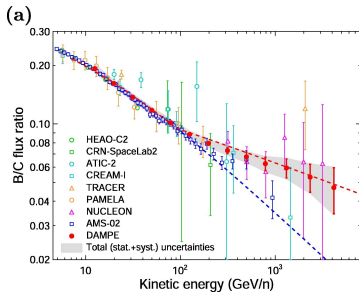
# Observations



- The overabundant elements show steeper spectra than the other nuclei
- Interpretation of these observations: The secondary CRs are produced via spallation of primaries

[AMS Collaboration 2021; <http://www.srl.caltech.edu>]



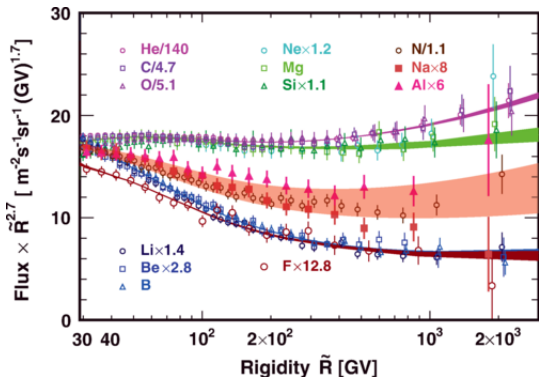


- Secondary over primary ratios let you infer a grammage = traversed column density of CRs on their way to Earth
- Energy dependent quantity
- Grammage can be related to the diffusion coefficient which in turn is connected to the microphysics and the magnetic turbulence in our Galaxy

[DAMPE Collaboration 2022]



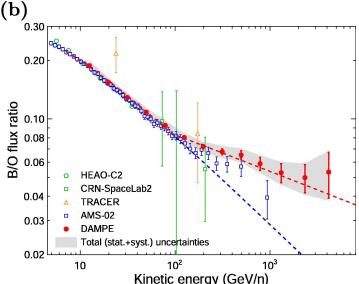
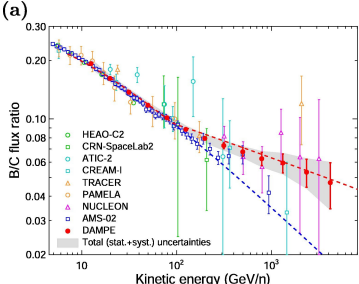
- Huge amount of data available by AMS-02



[AMS Collaboration 2021]

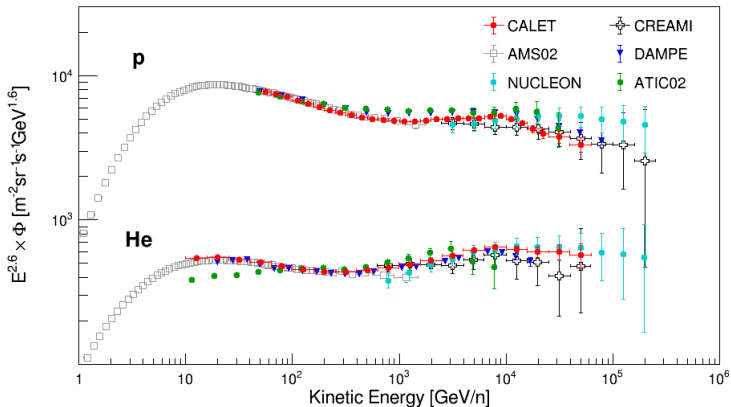


# Exciting Times



[DAMPE Collaboration 2022]



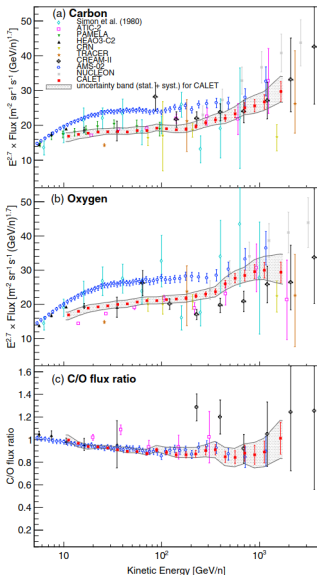


[CALET Collaboration 2023]





# There is a Problem



- The absolute fluxes of elements heavier than He show significantly different normalizations
- Makes a universal fit using data from different experiments more difficult

[CALET Collaboration 2020]



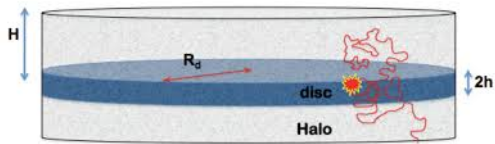
- These measurements led to many interesting discoveries:
  - Spectral hardening at 300 GV
  - Spectral softening around 10 TV
  - ...
- Each new measurement has the potential to unveil a new, unexpected aspect of CR transport which will ultimately lead to an increasingly complete picture
- Requires careful analysis of what is the origin of the feature, e.g., hardening due to a change of slope in  $D(E)$
- This can be motivated by a spatially dependent diffusion coefficient [Tomassetti 2012] or transition of scattering of self-generated to extrinsic turbulence [Blasi et al. 2012]



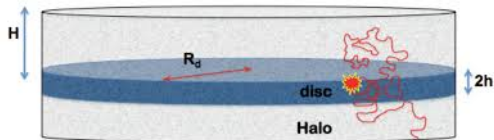
# Weighted Slab Model



# Standard Picture of CR Transport



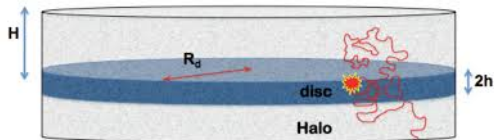
# Standard Picture of CR Transport



$$\begin{aligned}
 & -\frac{\partial}{\partial z} \left[ D_a \frac{\partial f_a}{\partial z} \right] + v_A \frac{\partial f_a}{\partial z} - \frac{dv_A}{dz} \frac{p}{3} \frac{\partial f_a}{\partial p} \\
 & + \frac{1}{p^2} \frac{\partial}{\partial p} \left[ p^2 \left( \frac{dp}{dt} \right)_{a,\text{ion}} f_a \right] + \frac{\mu v(p) \sigma_a}{m} \delta(z) f_a + \frac{f_a}{\hat{\tau}_{d,a}} \\
 = & 2h_d q_{0,a}(p) \delta(z) + \sum_{a' > a} \frac{\mu v(p) \sigma_{a' \rightarrow a}}{m} \delta(z) f_{a'} + \sum_{a' > a} \frac{f_{a'}}{\hat{\tau}_{d,a'}}
 \end{aligned}$$



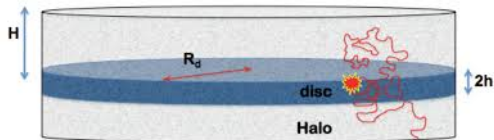
# Standard Picture of CR Transport



$$\begin{aligned}
 & \underbrace{-\frac{\partial}{\partial z} \left[ D_a \frac{\partial f_a}{\partial z} \right]}_{\text{Diffusion}} + v_A \frac{\partial f_a}{\partial z} - \frac{dv_A}{dz} \frac{p}{3} \frac{\partial f_a}{\partial p} \\
 & + \frac{1}{p^2} \frac{\partial}{\partial p} \left[ p^2 \left( \frac{dp}{dt} \right)_{a,\text{ion}} f_a \right] + \frac{\mu v(p) \sigma_a}{m} \delta(z) f_a + \frac{f_a}{\hat{\tau}_{d,a}} \\
 = & 2h_d q_{0,a}(p) \delta(z) + \sum_{a' > a} \frac{\mu v(p) \sigma_{a' \rightarrow a}}{m} \delta(z) f_{a'} + \sum_{a' > a} \frac{f_{a'}}{\hat{\tau}_{d,a'}}
 \end{aligned}$$



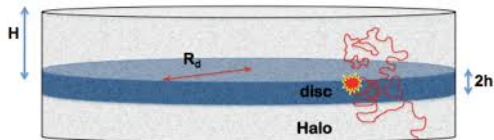
# Standard Picture of CR Transport



$$\begin{aligned}
 & \underbrace{-\frac{\partial}{\partial z} \left[ D_a \frac{\partial f_a}{\partial z} \right]}_{\text{Diffusion}} + \underbrace{v_A \frac{\partial f_a}{\partial z}}_{\text{Advection}} - \frac{dv_A}{dz} \frac{p}{3} \frac{\partial f_a}{\partial p} \\
 & + \frac{1}{p^2} \frac{\partial}{\partial p} \left[ p^2 \left( \frac{dp}{dt} \right)_{a,\text{ion}} f_a \right] + \frac{\mu v(p) \sigma_a}{m} \delta(z) f_a + \frac{f_a}{\hat{\tau}_{d,a}} \\
 = & 2h_d q_{0,a}(p) \delta(z) + \sum_{a' > a} \frac{\mu v(p) \sigma_{a' \rightarrow a}}{m} \delta(z) f_{a'} + \sum_{a' > a} \frac{f_{a'}}{\hat{\tau}_{d,a'}}
 \end{aligned}$$



# Standard Picture of CR Transport

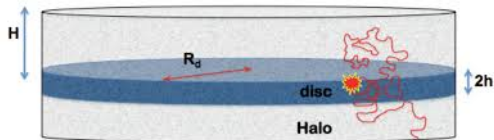


$$\begin{aligned}
 & \underbrace{-\frac{\partial}{\partial z} \left[ D_a \frac{\partial f_a}{\partial z} \right]}_{\text{Diffusion}} + \underbrace{v_A \frac{\partial f_a}{\partial z}}_{\text{Advection}} - \underbrace{\frac{dv_A}{dz} \frac{p}{3} \frac{\partial f_a}{\partial p}}_{\text{Adiabatic E-losses}} \\
 & + \frac{1}{p^2} \frac{\partial}{\partial p} \left[ p^2 \left( \frac{dp}{dt} \right)_{a,\text{ion}} f_a \right] + \frac{\mu v(p) \sigma_a}{m} \delta(z) f_a + \frac{f_a}{\hat{\tau}_{d,a}} \\
 = & 2h_d q_{0,a}(p) \delta(z) + \sum_{a' > a} \frac{\mu v(p) \sigma_{a' \rightarrow a}}{m} \delta(z) f_{a'} + \sum_{a' > a} \frac{f_{a'}}{\hat{\tau}_{d,a'}}
 \end{aligned}$$





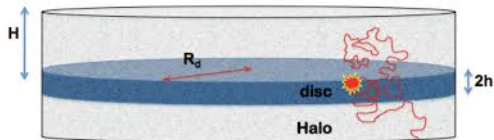
# Standard Picture of CR Transport



$$\begin{aligned}
 & \underbrace{-\frac{\partial}{\partial z} \left[ D_a \frac{\partial f_a}{\partial z} \right]}_{\text{Diffusion}} + \underbrace{v_A \frac{\partial f_a}{\partial z}}_{\text{Advection}} - \underbrace{\frac{dv_A}{dz} \frac{p}{3} \frac{\partial f_a}{\partial p}}_{\text{Adiabatic E-losses}} \\
 & + \underbrace{\frac{1}{p^2} \frac{\partial}{\partial p} \left[ p^2 \left( \frac{dp}{dt} \right)_{a,\text{ion}} f_a \right]}_{\text{Ionization losses}} + \frac{\mu v(p) \sigma_a}{m} \delta(z) f_a + \frac{f_a}{\hat{\tau}_{d,a}} \\
 = & 2h_d q_{0,a}(p) \delta(z) + \sum_{a' > a} \frac{\mu v(p) \sigma_{a' \rightarrow a}}{m} \delta(z) f_{a'} + \sum_{a' > a} \frac{f_{a'}}{\hat{\tau}_{d,a'}}
 \end{aligned}$$



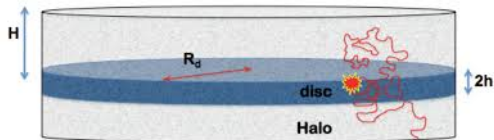
# Standard Picture of CR Transport



$$\begin{aligned}
 & \underbrace{-\frac{\partial}{\partial z} \left[ D_a \frac{\partial f_a}{\partial z} \right]}_{\text{Diffusion}} + \underbrace{v_A \frac{\partial f_a}{\partial z}}_{\text{Advection}} - \underbrace{\frac{dv_A}{dz} \frac{p}{3} \frac{\partial f_a}{\partial p}}_{\text{Adiabatic E-losses}} \\
 & + \underbrace{\frac{1}{p^2} \frac{\partial}{\partial p} \left[ p^2 \left( \frac{dp}{dt} \right)_{a,\text{ion}} f_a \right]}_{\text{Ionization losses}} + \underbrace{\frac{\mu v(p) \sigma_a}{m} \delta(z) f_a}_{\text{Spallation losses}} + \frac{f_a}{\hat{\tau}_{d,a}} \\
 = & 2h_d q_{0,a}(p) \delta(z) + \sum_{a' > a} \frac{\mu v(p) \sigma_{a' \rightarrow a}}{m} \delta(z) f_{a'} + \sum_{a' > a} \frac{f_{a'}}{\hat{\tau}_{d,a'}}
 \end{aligned}$$



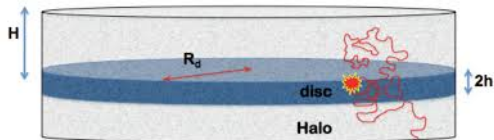
# Standard Picture of CR Transport



$$\begin{aligned}
 & \underbrace{-\frac{\partial}{\partial z} \left[ D_a \frac{\partial f_a}{\partial z} \right]}_{\text{Diffusion}} + \underbrace{v_A \frac{\partial f_a}{\partial z}}_{\text{Advection}} - \underbrace{\frac{dv_A}{dz} \frac{p}{3} \frac{\partial f_a}{\partial p}}_{\text{Adiabatic E-losses}} \\
 & + \underbrace{\frac{1}{p^2} \frac{\partial}{\partial p} \left[ p^2 \left( \frac{dp}{dt} \right)_{a,\text{ion}} f_a \right]}_{\text{Ionization losses}} + \underbrace{\frac{\mu v(p) \sigma_a}{m} \delta(z) f_a}_{\text{Spallation losses}} + \underbrace{\frac{f_a}{\hat{\tau}_{d,a}}}_{\text{Radioactive decay}} \\
 = & 2h_d q_{0,a}(p) \delta(z) + \sum_{a' > a} \frac{\mu v(p) \sigma_{a' \rightarrow a}}{m} \delta(z) f_{a'} + \sum_{a' > a} \frac{f_{a'}}{\hat{\tau}_{d,a'}}
 \end{aligned}$$



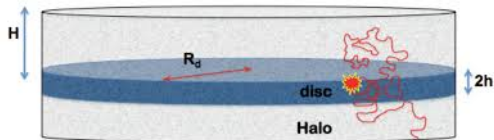
# Standard Picture of CR Transport



$$\begin{aligned}
 & \underbrace{-\frac{\partial}{\partial z} \left[ D_a \frac{\partial f_a}{\partial z} \right]}_{\text{Diffusion}} + \underbrace{v_A \frac{\partial f_a}{\partial z}}_{\text{Advection}} - \underbrace{\frac{dv_A}{dz} \frac{p}{3} \frac{\partial f_a}{\partial p}}_{\text{Adiabatic E-losses}} \\
 & + \underbrace{\frac{1}{p^2} \frac{\partial}{\partial p} \left[ p^2 \left( \frac{dp}{dt} \right)_{a,\text{ion}} f_a \right]}_{\text{Ionization losses}} + \underbrace{\frac{\mu v(p) \sigma_a}{m} \delta(z) f_a}_{\text{Spallation losses}} + \underbrace{\frac{f_a}{\hat{\tau}_{d,a}}}_{\text{Radioactive decay}} \\
 = & \underbrace{2h_d q_{0,a}(p) \delta(z)}_{\text{Injection at the sources}} + \sum_{a' > a} \frac{\mu v(p) \sigma_{a' \rightarrow a}}{m} \delta(z) f_{a'} + \sum_{a' > a} \frac{f_{a'}}{\hat{\tau}_{d,a'}}
 \end{aligned}$$



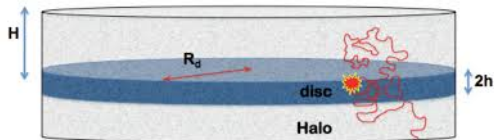
# Standard Picture of CR Transport



$$\begin{aligned}
 & \underbrace{-\frac{\partial}{\partial z} \left[ D_a \frac{\partial f_a}{\partial z} \right]}_{\text{Diffusion}} + \underbrace{v_A \frac{\partial f_a}{\partial z}}_{\text{Advection}} - \underbrace{\frac{dv_A}{dz} \frac{p}{3} \frac{\partial f_a}{\partial p}}_{\text{Adiabatic E-losses}} \\
 & + \underbrace{\frac{1}{p^2} \frac{\partial}{\partial p} \left[ p^2 \left( \frac{dp}{dt} \right)_{a,\text{ion}} f_a \right]}_{\text{Ionization losses}} + \underbrace{\frac{\mu v(p) \sigma_a}{m} \delta(z) f_a}_{\text{Spallation losses}} + \underbrace{\frac{f_a}{\hat{\tau}_{d,a}}}_{\text{Radioactive decay}} \\
 = & \underbrace{2h_d q_{0,a}(p) \delta(z)}_{\text{Injection at the sources}} + \underbrace{\sum_{a' > a} \frac{\mu v(p) \sigma_{a' \rightarrow a}}{m} \delta(z) f_{a'}}_{\text{Production via Spallation}} + \sum_{a' > a} \frac{f_{a'}}{\hat{\tau}_{d,a'}}
 \end{aligned}$$



# Standard Picture of CR Transport



$$\begin{aligned}
 & \underbrace{-\frac{\partial}{\partial z} \left[ D_a \frac{\partial f_a}{\partial z} \right]}_{\text{Diffusion}} + \underbrace{v_A \frac{\partial f_a}{\partial z}}_{\text{Advection}} - \underbrace{\frac{dv_A}{dz} \frac{p}{3} \frac{\partial f_a}{\partial p}}_{\text{Adiabatic E-losses}} \\
 & + \underbrace{\frac{1}{p^2} \frac{\partial}{\partial p} \left[ p^2 \left( \frac{dp}{dt} \right)_{a,\text{ion}} f_a \right]}_{\text{Ionization losses}} + \underbrace{\frac{\mu v(p) \sigma_a}{m} \delta(z) f_a}_{\text{Spallation losses}} + \underbrace{\frac{f_a}{\hat{\tau}_{d,a}}}_{\text{Radioactive decay}} \\
 = & \underbrace{2h_d q_{0,a}(p) \delta(z)}_{\text{Injection at the sources}} + \underbrace{\sum_{a' > a} \frac{\mu v(p) \sigma_{a' \rightarrow a}}{m} \delta(z) f_{a'}}_{\text{Production via Spallation}} + \underbrace{\sum_{a' > a} \frac{f_{a'}}{\hat{\tau}_{d,a'}}}_{\text{Production due to decay}}
 \end{aligned}$$

- $\sim 90$  coupled differential equations



- Same equation used by different groups with two different approaches: solving the equation numerically [Korsmeier & Cuoco 2021; Boschini et al. 2021; De La Torre Luque et al. 2022] or semianalytically [Evoli et al. 2019; Weinrich et al. 2020; Schroer et al. 2021]
- Big differences can arise from different cross-section models used
- Uncertainties in production cross sections of  $\sim 20 - 30\%$  are often limiting factor to reach conclusions
- Focus has been on elements lighter than O but since the release of AMS-02 data of heavier nuclei, the whole nucleus chain was incorporated into the models [Boschini et al. 2021; Schroer et al. 2021; De La Torre Luque et al. 2022]
- Main difference in our analysis: All primaries are injected with the same slope  $\gamma$ , expected at zeroth order from diffuse shock acceleration



One can rewrite as equation in terms of grammage and flux  $I_a(E) = 4\pi Ap^2 f_a(p)$ :

$$\frac{I_a(E)}{X_a(E)} + \frac{d}{dE} \left( \left[ \left( \frac{dE}{dx} \right)_{ad} + \left( \frac{dE}{dx} \right)_{ion,a} \right] I_a(E) \right) + \frac{I_a(E)}{X_{cr,a}} = 2h \frac{A_a p^2 q_a(p)}{\mu v} + \sum_{a' > a} \frac{I_{a'}(E)}{m} \sigma_{a' \rightarrow a}$$

- where we introduced the critical grammage  $X_{cr,a} := \frac{m}{\sigma_a}$  and the grammage traversed by nuclei a  $X_a(E) := \frac{\mu v}{2v_A} \left( 1 - e^{-\frac{v_A H}{D}} \right)$
- Solutions only sensitive to ratio  $\frac{H}{D}$
- Without energy losses  $I_a(E) \propto E^{-\gamma+2}$  for  $X_a(E) \gg X_{cr,a}$  and  $I_a(E) \propto E^{-\gamma+2-\delta}$  for  $X_a(E) \ll X_{cr,a}$
- $\Rightarrow$  Secondary over primary ratios flat at low E and  $\propto E^{-\delta}$  at high E





# Fitting Parameters

- Spatial transport, including diffusion and advection, comprises 7 free-parameters:  $D_0$ ,  $\delta$ ,  $v_A$ ,  $H$ ,  $R_b$ ,  $\Delta\delta$ ,  $s$ :

$$D(R) = 2v_A H + \beta D_0 \frac{(R/GV)^\delta}{[1 + (R/R_b)^{\Delta\delta/s}]^s},$$

motivated by [Recchia et al. 2016]

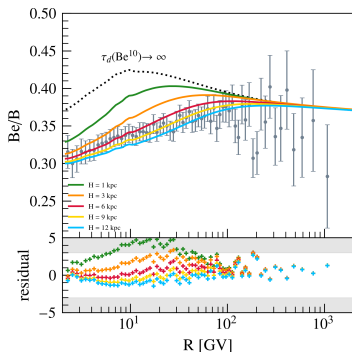
- Injection slope  $\gamma$ , assumed to be the same for all of them without any break
- The injection efficiencies  $\epsilon_a$  of the species H, He, C, N, O, Ne, Mg, Si, S and Fe
- Solar modulation potential  $\phi$
- Total of 19 parameters
- Restrict ourselves to  $R > 10$  GV to reduce the impact of low-energy effects



# Lighter Nuclei



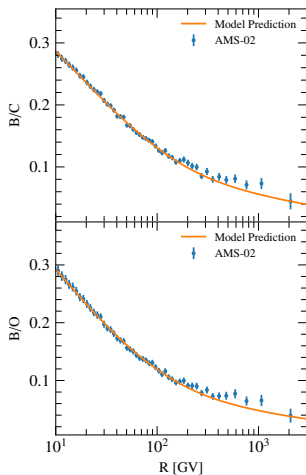
# Determining the Halo size



- For radioactive nuclei  $X_a(E) \approx \frac{\mu V}{2} \sqrt{\frac{\tau_d}{D}}$  for  $\tau_d \ll \min\left(\frac{H^2}{D}, \frac{H}{v_A}\right)$
- With our model a Halo size  $H \geq 5$  kpc is preferred [Evoli et al. 2020]
- Influenced by cross section uncertainties
- Compatible within uncertainties with  $\sim 5$  kpc found by [Weinrich et al. 2020] and  $\sim 4$  kpc by [Boschini et al. 2020; Maurin et al. 2022]
- In the following, we fix  $H = 7$  kpc in our model



# Fit to light Ratios



[Schroer et al., 2021]

Benedikt Schroer (UChicago)

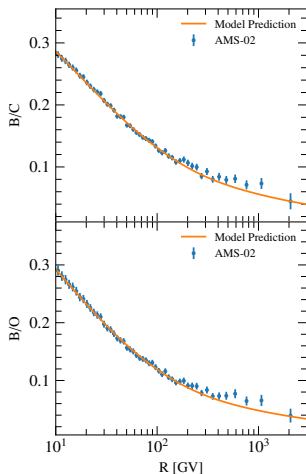
CRA Workshop 2023

May 16, 2023

15 / 26



# Fit to light Ratios

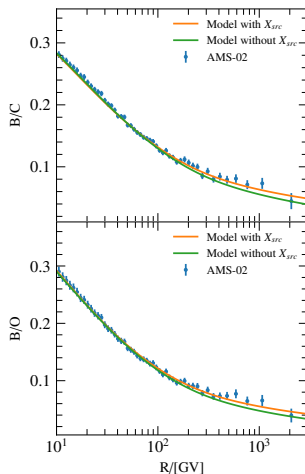
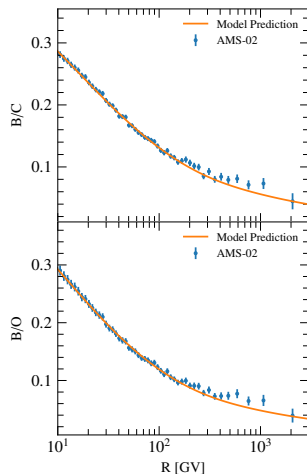


- Source grammage or reacceleration can improve agreement at high energies [Evoli et al. 2019; Bresci et al. 2019]

[Schroer et al. 2021]



# Fit to light Ratios

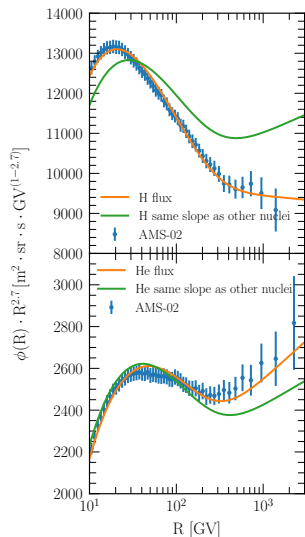


- Source grammage or reacceleration can improve agreement at high energies [Evoli et al. 2019; Bresci et al. 2019]
- Even more important at higher energies probed by DAMPE and CALET

[Schroer et al. 2021]



# He and H Results



[Schroer et al. 2021]

- H and He require a different slope than other nuclei and each other, confirms result of previous study [Evoli et al. 2019] and independently confirmed by [Weinrich et al. 2020]
- Puzzling result as even theories that explain different slope of H and He predict same slope of He and heavier nuclei [Malkov et al. 2012]
- Raises the question: Is there an observable trend of the acceleration slope with particle mass?

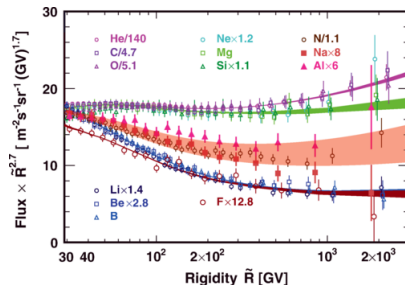


# Intermediate-mass and Heavy Nuclei





# Intermediate-Mass Nuclei

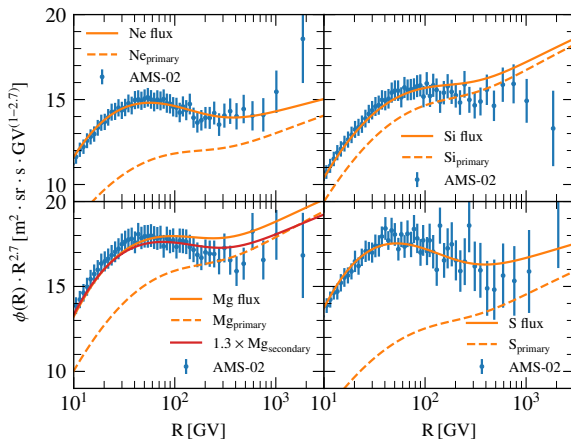


- AMS-02 measures different slopes for different nuclei
- Good fits have been achieved using different injection slopes for different primary CRs [Boschini et al. 2020; De La Torre Luque et al. 2022]
- However, is it possible to fit the data using the same injection slope?

[AMS Collaboration 2021]



# Our Results

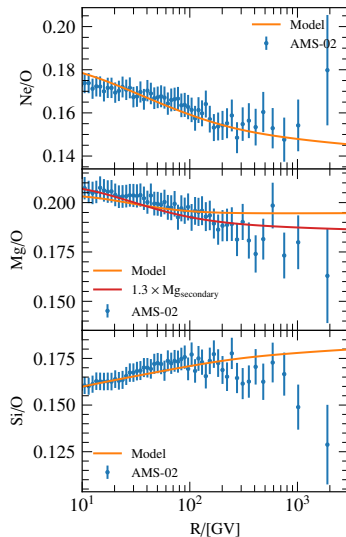
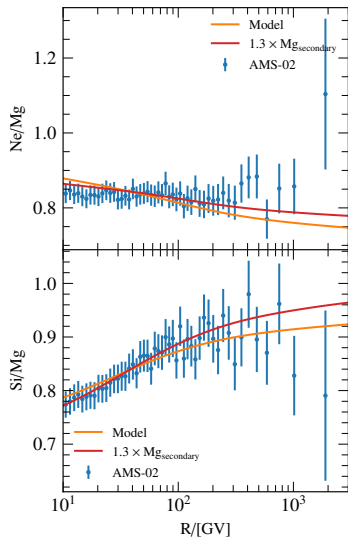


- Requiring the same slope leads to reasonably good fits
- Possible tensions can be lifted with cross-section uncertainties (see Mg) and possibly source grammage plays a role as well

[Schroer et al. 2021]



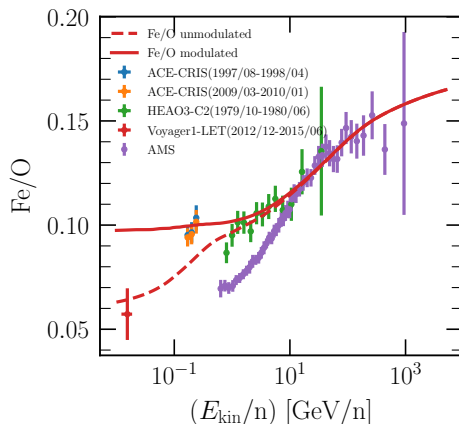
# Fit to the Ratios



[Schroer et al. 2021]



# One Exception

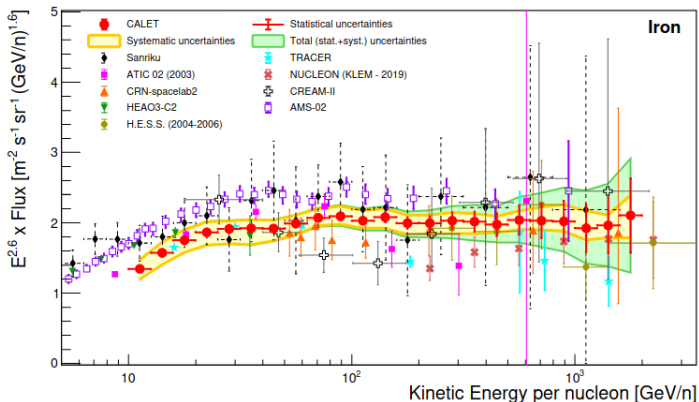


- Our model is compatible with all available data except AMS-02
- Fe data might require to incorporate a new or so far neglected effect into our model

[Schroer et al. 2021]



# CALET Fe Measurement



- CALET measurement shows different normalization than AMS-02, but confirms slope
- However does not cover the part of the spectrum where we see the large deviations from our model and other experiments

[CALET Collaboration 2021]



We tested different possible shortcomings of our model:

- Iron suffers severe energy losses, maybe ionization or spallation are not properly accounted for.



We tested different possible shortcomings of our model:

- ~~Iron suffers severe energy losses, maybe ionization or spallation are not properly accounted for.~~ Ionization has to be 5 times higher or spallation 40% larger to obtain a somewhat better fit
- The spallation inside the halo could become important



We tested different possible shortcomings of our model:

- ~~Iron suffers severe energy losses, maybe ionization or spallation are not properly accounted for.~~ Ionization has to be 5 times higher or spallation 40% larger to obtain a somewhat better fit
- ~~The spallation inside the halo could become important~~ Effect of halogrammage stays of %-order for reasonable halo densities
- Maybe iron experiences slightly different solar modulation for some unknown reason.





We tested different possible shortcomings of our model:

- ~~Iron suffers severe energy losses, maybe ionization or spallation are not properly accounted for.~~ Ionization has to be 5 times higher or spallation 40% larger to obtain a somewhat better fit
- ~~The spallation inside the halo could become important~~ Effect of halogrammage stays of %-order for reasonable halo densities
- ~~Maybe iron experiences slightly different solar modulation for some unknown reason.~~ Iron would need a 70% stronger modulation potential without any theoretical motivation
- Iron could have another injection slope

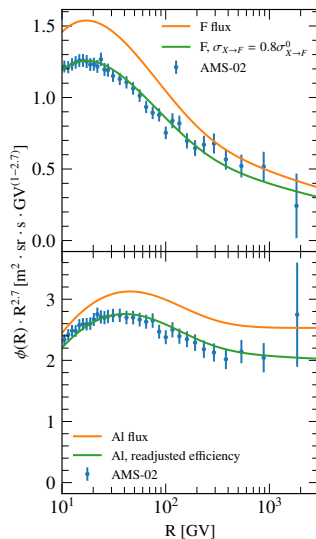
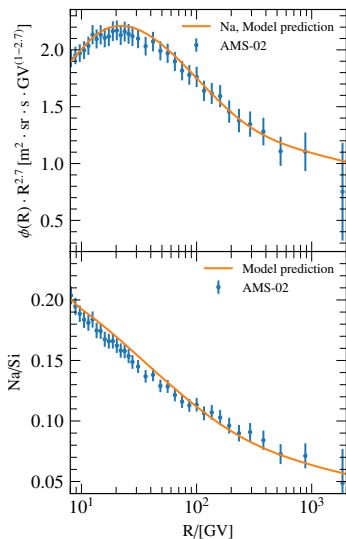


We tested different possible shortcomings of our model:

- ~~Iron suffers severe energy losses, maybe ionization or spallation are not properly accounted for.~~ Ionization has to be 5 times higher or spallation 40% larger to obtain a somewhat better fit
- ~~The spallation inside the halo could become important~~ Effect of halogrammage stays of %-order for reasonable halo densities
- ~~Maybe iron experiences slightly different solar modulation for some unknown reason.~~ Iron would need a 70% stronger modulation potential without any theoretical motivation
- ~~Iron could have another injection slope~~ Does not give a satisfying fit either



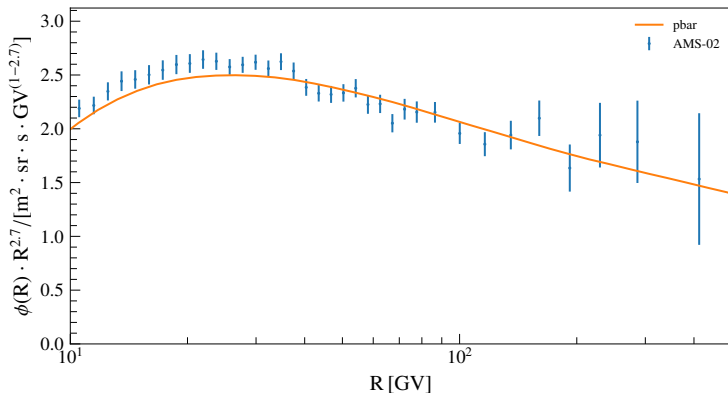
# Model Predictions vs. Measurements



- Prediction for Na agrees perfectly while Al and F require slight modifications



# Preliminary Results for Antiprotons



- We use the up-to-date, differential cross section by [Korsmeier et al. 2018]
- Preliminary results seem promising, no need of new physics



## Conclusion and Outlook



# Conclusion

- Many different groups with similar approaches able to fit AMS-02 data of lighter nuclei
- Cross section uncertainties play an important role for detecting physical anomalies
- Our model is able to reproduce flux of all intermediate-mass to light elements using a single injection slope for all nuclei heavier than He reducing heavily the amount of free parameters compared to other studies like [Boschini et al. 2020; De La Torre Luque et al. 2022] who fit all nuclei simultaneously
- Able to give predictions which are compatible with new data without refitting the model
- There seems to be an issue with Fe, that we still need to understand



- New Measurements of CALET and DAMPE will allow for independent check of transport parameters and might unveil importance of additional effects such as source grammage or reacceleration due to higher energy range
- Future measurement of  $\text{Be}^{10}/\text{Be}^9$  by HELIX and AMS-02 will allow for a more precise determination of the halo size, although cross section uncertainties might become the limiting factor



# Backup Slides





$$\begin{aligned} \frac{I_a(E)}{X_a(E)} + \frac{d}{dE} \left( \left[ \left( \frac{dE}{dx} \right)_{ad} + \left( \frac{dE}{dx} \right)_{ion,a} \right] I_a(E) \right) \\ + \frac{I_a(E)}{X_{cr,a}} = 2h \frac{A_a p^2 q_a(p)}{\mu v} + \sum_{a' > a} \frac{I_{a'}(E)}{m} \sigma_{a' \rightarrow a} \\ \Rightarrow \Lambda_{1,a}(E) I_a(E) + \Lambda_{2,a}(E) \partial_E I_a(E) = Q_a(E) \end{aligned}$$

Solution:

$$I_a(E) = \int_E dE' \frac{Q_a(E')}{|\Lambda_{2,a}(E')|} \exp \left[ - \int_E^{E'} dE'' \frac{\Lambda_{1,a}(E'')}{|\Lambda_{2,a}(E'')|} \right]$$

code solves iteratively this equation starting from the heaviest isotope

~ 90 different isotopes from Ni-64 to H

